Nature Environment and Pollution Technology
An International Quarterly Scientific Journal

p-ISSN: 0972-6268
(Print copies up to 2016)
e-ISSN: 2395-3454

Vol. 21 | No. 2 | pp. 517-527 | 2022

Original Research Paper

https://doi.org/10.46488/NEPT.2022.v21i02.010

Open Access Journal

Study on the Effect of Shrubs on Wind Erosion Control in Desert Regions

Naqi Lessani*, Hanfeng Wang*† and Ahmad Hamed Nikmal**
*School of Civil Engineering, Central South University, Changsha, P. R. China
**School of Civil Engineering and Environment, University of Science and Technology, Beijing, P. R. China
†Corresponding author: Hanfeng Wang; wanghf@csu.edu.cn

Nat. Env. & Poll. Tech.
Website: www.neptjournal.com

Received: 05-05-2021
Revised: 26-06-2021
Accepted: 15-07-2021

Key Words:
Numerical simulation
Wind erosion control
Vegetation
Shelterbelt
Windblown sand

ABSTRACT

The wind velocity reduces by encountering vegetation; thus, a shelter zone is generated at downstream of vegetation. Hence, planting vegetation, mainly shrubs, has widely been used to control sand transportation. However, plant shrubs in a large area of the desert are practically unsustainable and uneconomical. In this study, Computational Fluid Dynamic (CFD) and wind tunnel experiments were carried out to optimize the planting method of shrubs that could decrease the number of shrubs and increase wind erosion controlling efficiency in desert regions. The effects of shrub height, porosity, the number of shrub rows, and space between shrub rows on wind erosion control were studied. Based on the present study results, the downstream of shrubs was divided into three different zones: first erosion zone, sedimentation zone, and second erosion zone. Moreover, with the increase of shrub porosity, the first erosion zone's length increased. In contrast, the sedimentation zone's length decreased, whereas the length of the first erosion and sedimentation zones increased with shrub height. Hence, to make a better shelter zone, it is recommended to plant denser shrubs rows at the upstream and sparsely shrub rows at the far downstream.

INTRODUCTION

Vegetations have over time been used to control wind erosion in desert regions near infrastructures, particularly railway lines located in desert regions. Human activities and climate change have intensified the rate of desertification surges (Qu et al. 2007). Wind erosion occurs in arid and semi-arid regions, negatively affecting the environment and the infrastructures (Prospero 1999, Griffin et al. 2001, Lv & Dong 2012, Cheng et al. 2017). Sandstorms cause huge damage to infrastructures (Yao et al. 2012, Sarkar et al. 2019).

Vegetations have been considered to be effective in controlling wind erosion (Hong et al. 2020). Trees and shrubs have widely been used to create shelterbelts. However, in desert regions, shrubs have proven to be more likely employed than trees, and shrubs can survive in conditions with limited moisture and nutrients (Zhang 1994, Xu 1996, Lv & Dong 2012).

The morphology of shrubs and the arrangement are significant features that govern wind velocity reduction effectiveness: Porosity, shape, height, configuration, thickness, spacing, shrub coverage are factors that determine the efficiency of vegetations shelterbelt in wind erosion control (Cornelis & Gabriels 2005, Lv & Dong 2012, Jian et al. 2018, Liu et al. 2018).

An additional row of the tree has a significant effect on wind velocity reduction, which is almost twice (Rosenfeld et al. 2010). Wind mitigation zones are better provided by trees with large bottoms and narrow tops. In actuality, most trees have a narrow bottom and a wide top, resulting in a considerable rise in the total shelterbelt effect coverage percentage. Single plants, on the other hand, have a lower efficiency (Liu et al. 2018). Sand transportation is reduced by 92 percent when grasses grow to cover 28 percent of the ground surface (Ash & Wasson 1983).

In straw checkboard systems, vegetation such as reeds, wheat, saxual tree, and other plants are planted. A square-shaped straw checkboard measuring 1 m by 1 m reduces wind velocity and stabilizes sand delivery (Station 1986). The best wind reduction efficiency and dune fixing were observed with a 10 cm to 20 cm height with a 1 m by 1 m square straw checkboard (Qiu et al. 2004). In a small-sized straw checkboard, sand transportation rate varies logarithmically, and in the large-sized straw checkboard, sand transportation rate and wind velocity vary exponentially (Gao et al. 2004). The height and density, which are split into three zones, have a major impact on the variation of wind field characteristics at the leeward of the straw checkboard barrier belt (Qu et al. 2007). The wind velocity on both sides of the straw checkboard barrier decreased and a formula was developed to estimate the straw checkboard barrier's lifetime (Bo et al. 2015).

The technology of computational fluid dynamics (CFD) has been widely employed to study the aerodynamics and

characteristics of porous media (Bitog et al. 2009, Jian et al. 2018). To simulate porous material in the CFD approach, an additional term is introduced to the momentum equation (Li et al. 2006, Yoshida 2006, Mochida et al. 2008). The result of an experiment and a CFD simulation of a porous fence with a well-fitting k-turbulence model (Santiago et al. 2007). Previous research has shown that CFD simulation can accurately predict flow characteristics near vegetation (Guo & Maghirang 2012).

The majority of previous researches focused on vegetation coverage and wind erosion control. However, few studies focused on recommending the plantation design of shrubs as a function of height, porosity, row spacing and a number of rows on wind erosion control. In this study, based on the threshold friction velocity, the shrub's downstream is divided into the first erosion zone, sedimentation zone and second erosion zone. The effect of shrub height, porosity, the number of rows and the shrub rows space on each zone were studied in details. The specific objective of this study is to determine the length of each zones as function of shrubs height, porosity. Thus, the best space between each rows of shrubs can be recommended for planting, which decrease the total number of shrubs, but at the same time increase sand controlling efficiency in desert regions.

Threshold Friction Velocity

Threshold friction velocity is the minimum friction velocity that lifts off the sand particles from the ground surface. It depends on soil properties such as soil texture, salt content, moisture content, and surface characteristics (Shao & Lu 2000). An empirical formula that describes a relationship between threshold friction velocity, friction velocity, and particles diameter was developed the formula is presented in equation (1) (Tsoar 1994).

$$u_{*_t} = A\sqrt{\frac{\rho_p - \rho}{\rho} gd} \quad \text{... (1)}$$

Where u_{*t} is the threshold friction velocity, A is a constant which is equal to 0.01, ρ_p is the density of sand, ρ is the density of air, and g is the gravitational acceleration.

The Bagnold formula is another name for the formula. It accurately predicts the friction velocity of particles larger than 0.1 mm. It is, however, unable of predicting the size of particles smaller than 0.075 mm. To address this deficiency, a formula was devised that took into account both cohesive force and aerodynamic lift, as shown in equation (2) (Thomas 1988).

$$u_{*_t} = A\sqrt{\sigma_p gd}F(R_{e_{*_t}})G(D)\sqrt{b^2 - 4ac} \quad \text{... (2)}$$

A, F and G are coefficients obtained from the wind tunnel; F is a function of the particles Reynold number at threshold friction velocity; whereas σ_p is the ratio of the densities of particles to the air.

As shown in Equation (3), a formula was developed that follows Bagnold's formula with an additional coefficient that incorporates sediment moisture in terms of cohesive force (Dong et al. 2007). It was estimated that the wind velocity for sand transportation in the desert region is 12 m.s^{-1} (Wu & Zhang 2012).

$$u_{*_t} = 0.16\sqrt{\frac{\rho_p - \rho_a}{\rho_a} gd}(1 + 478.20w^{1.52}) \quad \text{... (3)}$$

Where, w is the moisture content.

MATERIALS AND METHODS

Numerical Simulation

Governing equation: The two-dimensional turbulent incompressible transient flow was modeled around the shrub. The mass and momentum equations are solved in form of the Reynolds Averaged Navier Stokes (RANS) equations which is given as:

$$\frac{\partial u_i}{\partial x_i} = 0 \quad \text{... (4)}$$

$$\rho u_j \frac{\partial u_i}{\partial x_j} = -\frac{\partial p}{\partial x_i} + \frac{\partial}{\partial x_j}(\mu \frac{\partial u_i}{\partial x_j}) + S \quad \text{... (5)}$$

An additional source term is added in the momentum equation to represent the porous medium's momentum sink. The additional source term (S_i) in the whole flow domain is set to zero, except inside the shrubs. The additional source term could be written as follows:

$$S_i = (\frac{\mu}{a}\upsilon + c_2 \frac{1}{2}\rho\upsilon^2) \quad \text{... (6)}$$

Where C_2 is the inertial resistance; v is the magnitude of wind velocity; ρ is the density of air and α is the aerodynamic porosity. The first term in equation (6) can be ignored (Bitog et al. 2011). The second term is the inertial resistance for a porous media which can be defined as (Guo & Maghirang 2012):

$$c_2 = \frac{k_r}{w} \quad \text{... (7)}$$

Where k_r is the drag coefficient and w is the width of shrubs.

Simulation Setup

The shrub's height ranges from 0.2 to 2 meters. The size of the computational domain was set to be 120H in length and 20H in height, where H is the shrub's height. The typical K-epsilon turbulence model was used, along with a wall function. The entrance velocity profile, which is the logarithmic profile specified in Equation, was used (8).

$$u_{in} = \frac{u_*}{k} \ln(\frac{z}{z_0}) \quad \ldots (8)$$

Where u_{in} is the incoming flow velocity at height z ($m.s^{-1}$), where z is the height from the ground (m), K is the von Karman constant, and is friction velocity far upstream, which in this simulation 7 $m.s^{-1}$ and 20 $m.s^{-1}$ were applied.

Equations (9) and (10) were used to obtain the inlet's turbulent kinetic energy and turbulent dissipation rate.

$$\varepsilon_{in} = \frac{u_*^2}{kz} \quad \ldots (9)$$

$$k_{in} = \frac{u_*^2}{\sqrt{c_u}} \quad \ldots (10)$$

Where u_* is friction velocity far upstream.

Wind Tunnel Setup

The wind tunnel test was conducted to measure wind velocity at the downstream of Cedar shrub for obtaining its aerodynamic porosity, and at the same time validate the results of the CFD simulation. The experiment was carried out in Central South University's School of Civil Engineering's open circuit small wind tunnel laboratory.

Three Cedar shrubs with an average height of 20 cm, widths of 15 cm, 20 cm, and 15 cm from up to the downside of the shrub respectively, were distributed linearly in the wind tunnel.

A 2 cm thick Tongger desert sand was laid around the Cedar shrub in the test section of the wind tunnel. The sand bed surface was flattened using a steel ruler to make sure uneven surfaces were removed. The sand diameter used in this experiment varied from 0.5 mm to 1 mm. To evaluate the effect of different wind velocities on sand transportation, three different wind velocities 7 $m.s^{-1}$, 11.0 $m.s^{-1}$, and 20 $m.s^{-1}$, were applied. Then, sand transportation was observed around the single row of the shrubs. Fig. 1 shows the sand bed before the wind was blown.

RESULTS AND DISCUSSION

Wind Tunnel Measurement and Observation

The wind velocity at the downstream was measured using a hotwire anemometer. Cedar shrub's aerodynamic porosity; which is downstream over the upstream wind velocity, is calculated as shown in Fig. 3(a). Due to the acceleration of wind velocity between two columns of Cedar shrub, sand particles are transported through the gap between two-column of Cedar shrub downstream as shown in Fig. 2 (b). In this case, the incoming wind velocity was set to 11 m/s, which is below the threshold friction velocity for sand transportation.

Due to the Cedar shrub's presence, when sand particles collide with the shrubs, part of the sand particles rebound, and are deposited at the windward of the Cedar shrub, while the majority of particles pass over or through the shrubs. Fig. 2 (c) and (d) show the sand transportation at the windward, and leeward sides of the Cedar shrubs under 20 $m.s^{-1}$ wind velocity. As shown in Fig. 2(c), sand particles were deposited on the windward side. However, sand particles at the leeward side were swept away to about a distance of 1.4 m. Also, from Fig. 2(d) it can be observed that sand particles at the leeward, 1.4 m away from the Cedar shrubs, began sedimentation. This can be attributed to the change of wind velocity at the leeward side of a porous shelterbelt.

Numerical Analysis

In this section, the results obtained from the CFD simulations in the previous section are discussed.

Shrub porosity: 7 $m.s^{-1}$ wind velocity was employed to obtain the leeward wind velocity of Cedar shrub and compare it against the wind tunnel test data. For the rest of the simulation, 20 $m.s^{-1}$ wind velocity was used.

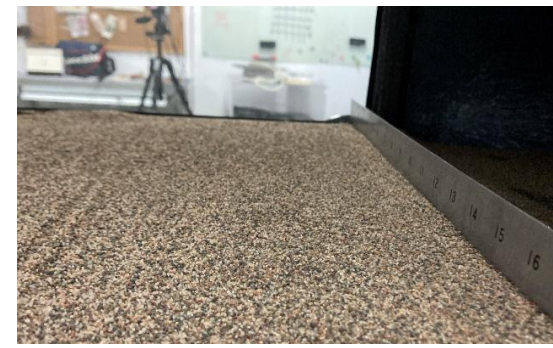

Fig. 1: Sandbed in the wind tunnel test section.

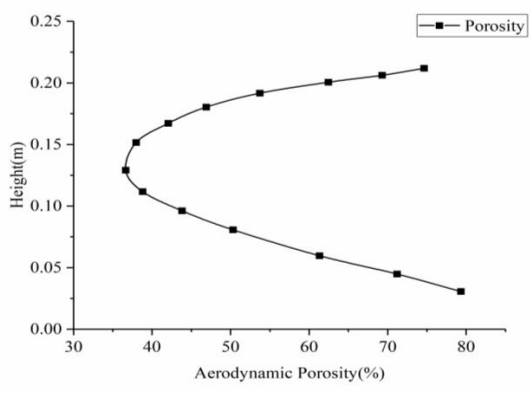

(a)

(b)

(c)

(d)

Fig. 2: (a) Aerodynamic porosity of Cedar shrub obtained in a wind tunnel (b) Sand transportation at leeward of Cedar shrub under 11 $m.s^{-1}$ (c) And (d) Show the sand transportation at the upstream, and downstream side of the Cedar shrub under 20 m/s wind velocity respectively.

The wind velocity at the leeward the surface is high as shown in Fig. 3(a), due to the high porosity at the bottom of Cedar shrub and low porosity at its middle. Also, the results obtained by CFD simulation, and wind tunnel measurement are virtually in good agreement. Fig. 3(b) shows that the wind velocity at a relative distance of 1.4 m, the wind velocity dropped to under 12 $m.s^{-1}$, which is the threshold friction velocity.

The wind velocity at the leeward gradually decreases, which reached its lowest value at a relative distance of 2 m. From a relative distance of 2 m to 3 m, the wind velocity is constant, and from a relative distance of 3 m above, the wind velocity began the recovery stage. Wind velocity at heights of 10 cm, and 18 cm share the same characteristics, which make a parabolic-shaped curve.

Fig. 3(b), Fig. 2(c), and (d) illustrate an appropriate correlation between near-surface wind velocity and

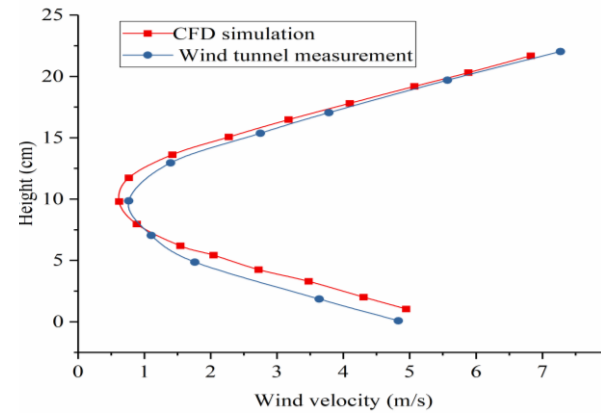

(a)

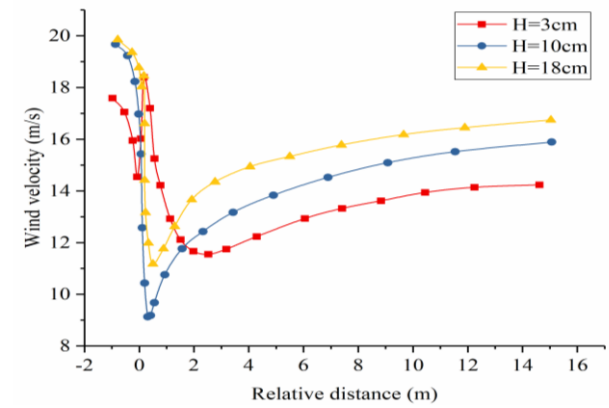

(b)

Fig. 3: (a) The vertical leeward wind velocity of Cedar shrub, x/h=0.5 (b) Horizontal wind velocity at three different heights from the ground surface.

Table 1: Erosion and sedimentation zones length for a 0.2 m high shrub.

Zone (m) Porosity (%)	L_e	L_a
60.0	Complete erosion zone	No sedimentation zone
50.0	Complete erosion zone	No sedimentation zone
40.0	1.4	2.7
30.0	0.8	5.0
15.0	0.6	6.0

sedimentation (Gao et al. 2004). Between relative distances 0 m and 1.4 m, the wind velocity exceeded the threshold friction velocity. Therefore, compared to Fig. 2(d), it can be seen that no sedimentation occurs at this distance. Consequently, using the characteristics of wind velocity is a proper method of evaluating sand transportation. Fig. 3(b) shows that the near-surface wind velocity at the downstream side can be divided into three zones: the first erosion zone L_e, sedimentation zone, and second erosion zone L_a. The length of these three zones depends on many factors such as incoming wind velocity, porosity, and height of the shrub. The three zones are illustrated in Fig. 4.

The first erosion zone is the distance where the wind velocity exceeds the threshold friction velocity. The sedimentation zone is the distance where the wind velocity is below threshold friction velocity.

It is essential to determine the length of the first erosion zone, and sedimentation zone as a function of shrub porosity. In Fig. 5, the grey color shows the sedimentation zone. As can be seen that the length of the first erosion zone increases with the decrease in porosity. When the porosity is beyond 40%, no sedimentation zone is generated.

The length of the first erosion zones for a shrub with 40%, 30%, and 15% porosity is 1.4 m, 0.8 m, and 0.6 m respectively. While the length of the sedimentation zones is 2.7 m, 5 m, and 6 m, respectively. Increasing the porosity decreases the length of the sedimentation zone.

Fig. 6(a) shows that shrub with low porosity has better wind velocity reduction where the first erosion zone is short, whereas the sedimentation zone is large.

Shrubs with porosity higher than 40% have wind velocity reduction; however, the wind velocity exceeds the threshold friction velocity. From Fig. 6(b) can be seen that the wind velocity at downstream near the surface is high. This is due to the high porosity of the shrub at the bottom and low porosity in the middle. Therefore, generally, because of this phenomenon, the first erosion zone occurs downstream. For cases in which the porosity of the shrub is less than 40 %, thus the sedimentation zone is generated.

Fig. 7(a), and (b) show shrub with 0.4 m height, 15%, 30%, and 40% porosity have 0.7 m, 0.9 m, 2 m first erosion zone length, while it has 14 m, 10 m, and 5 m sedimentation zone respectively. For this case, when the shrub porosity is beyond 40%, no sedimentation zone is generated, rather a

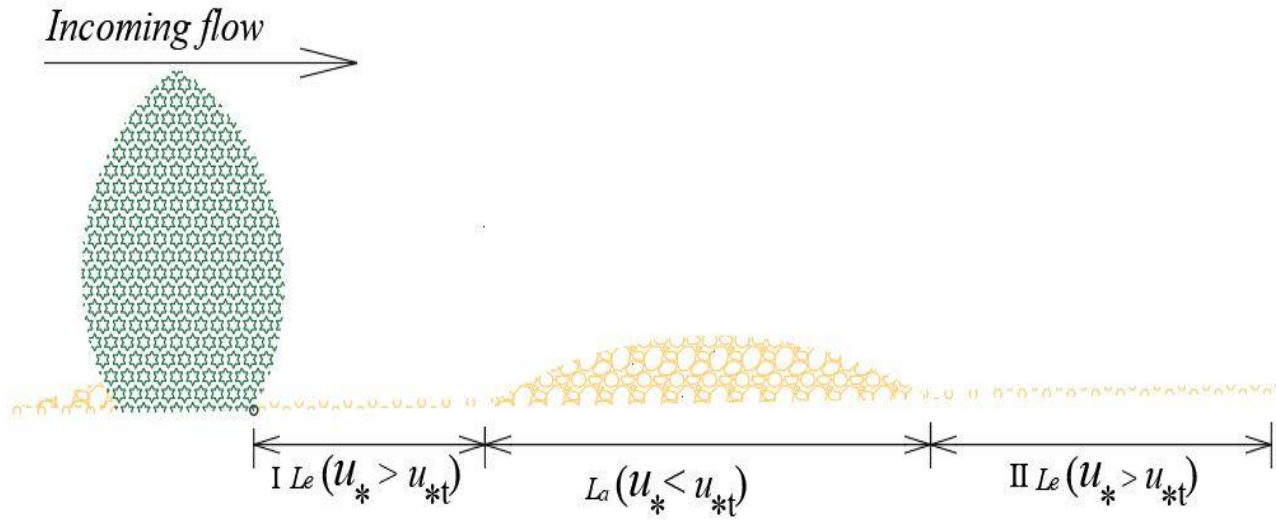

Fig. 4: Erosion zones and sedimentation zone.

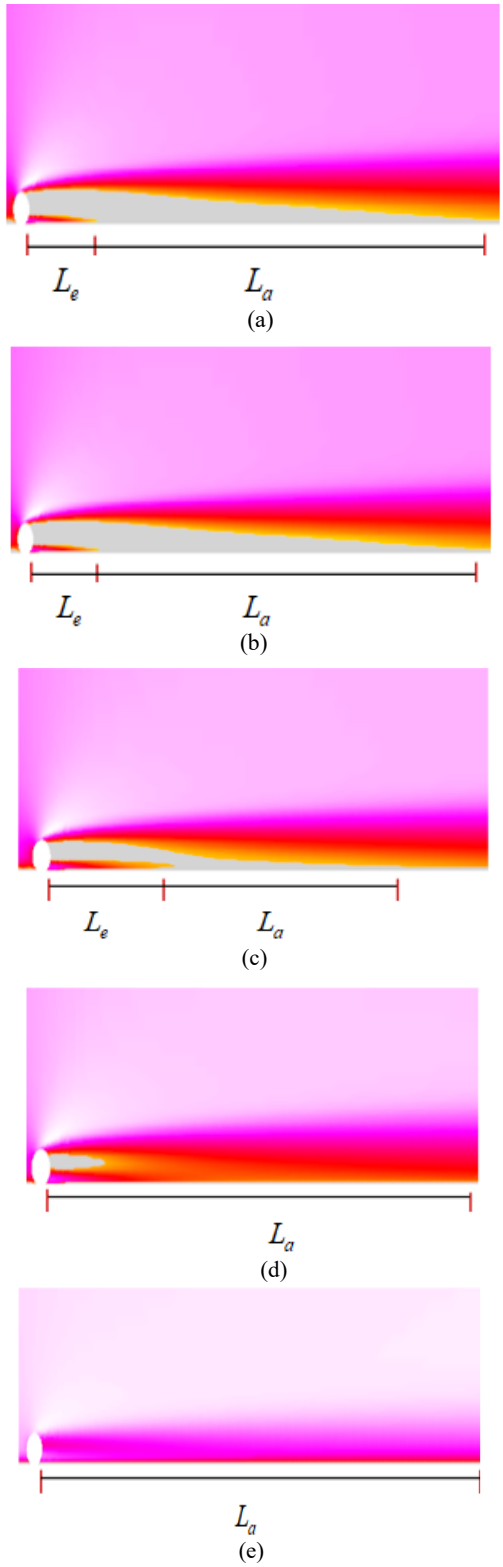

Fig. 5: Erosion zone and sedimentation zones of a 20 cm height shrub: (a) ϕ=15 %. (b) ϕ=30 %. (c) ϕ=40 %. (d) ϕ=50 %. (e) ϕ=60 %.

complete erosion zone was observed. For the shrub with 0.6 m height and 15%, 30%, 40%, and 50% porosity, the length of the first erosion zones are 0.8 m, 1.4 m, 2.5 m, and 4 m, respectively whereas, the length of sedimentation zones is 25 m, 18.5 m, 11.5 m and 6 m. Also, in this case for a shrub with porosity greater than 50 %, no sedimentation zone exists and likewise, for the 2 m height shrub with porosity greater than 60 %, no sedimentation zone is generated.

There is no sedimentation zone when the porosity of the shrub is greater than 40% for shrubs of 0.2 m and 0.4 m in height. No sedimentation zone is created if the porosity of a shrub with a height of 0.6 m, 0.8 m, or 1.2 m exceeds 50%, and if the porosity of a shrub with a height of 2 m surpasses 60%. As a result of the increased porosity and height, the length of the initial erosion zone increases. The length of the sedimentation zone, on the other hand, increases as the height and porosity decrease.

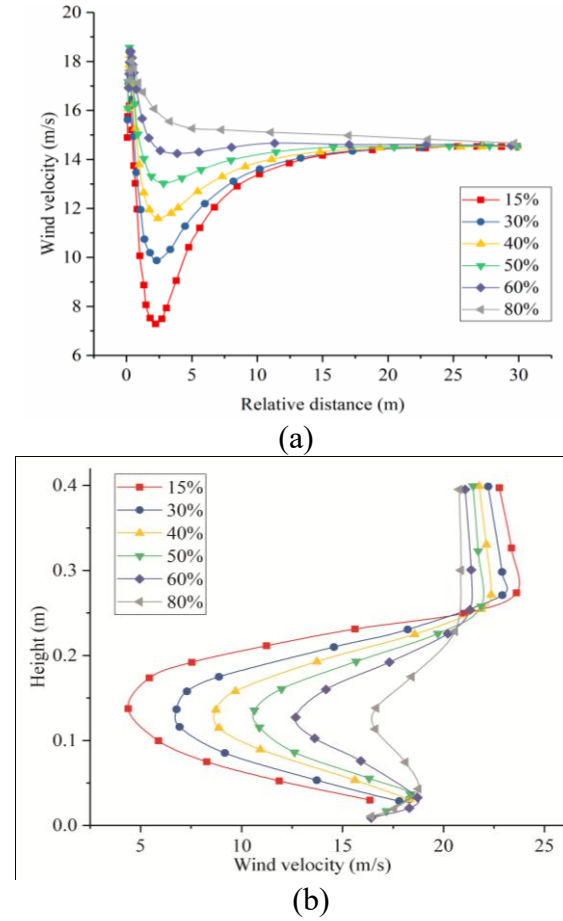

Fig. 6: (a) Horizontal wind velocity at height y =0.03 m and (b) Vertical wind velocity at relative distance x =0.1 m.

Shrub height: The shrub's height is one of the most critical factors that affect the characteristics of wind patterns at the leeward. The model with geodesic dome-shaped, and six different heights was simulated. Fig. 9 and 10 show plots of leeward vertical and horizontal wind velocity at x = 0.1 m, and y = 0.03 m, respectively. The wind velocity at the near ground surface decreases less, which is due to the high porosity of the shrub at the bottom. The biggest reduction in wind velocity happens near the middle of the shrub, though. As shown in Fig. 10, the highest horizontal wind velocity reduction for all porosity situations near the surface occurs at roughly 10h.

From Table 4, can be observed that by increasing shrub height, the length of the first erosion zone enlarges, and the length of the sedimentation zone also significantly enlarges. As the shrub porosity exceeds 50 % for a shrub with 0.2 m and 0.4 m height, a full erosion phenomenon occurs with no sedimentation zone. If the porosity exceeds 60% for shrubs shorter than 2 m, no sedimentation zone is generated. A shrub with 60% porosity and 2 m height has an 18 m sedimentation zone, while for a shorter shrub for the mentioned porosity, no sedimentation zone is generated (Fig.8).

Effect of rows number and space: Generally, shrubs with high porosity have a lesser effect on wind velocity reduction. 0.4 m high shrub with 70 %, and 80 % porosity with the different number of rows and rows spacing were simulated. First, the distance between single, double, triple, and four rows was set at 0.4 m. After evaluating wind velocity

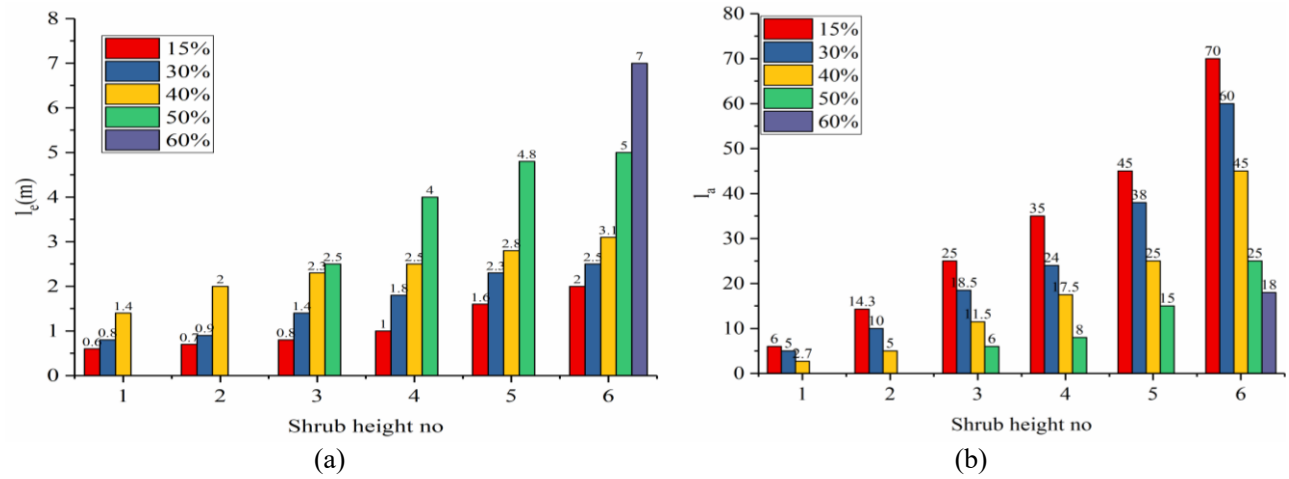

Fig. 7: L_e and L_a (a) Shrub porosity and first erosion zone length (b) Shrub porosity and sedimentation zone length (m).

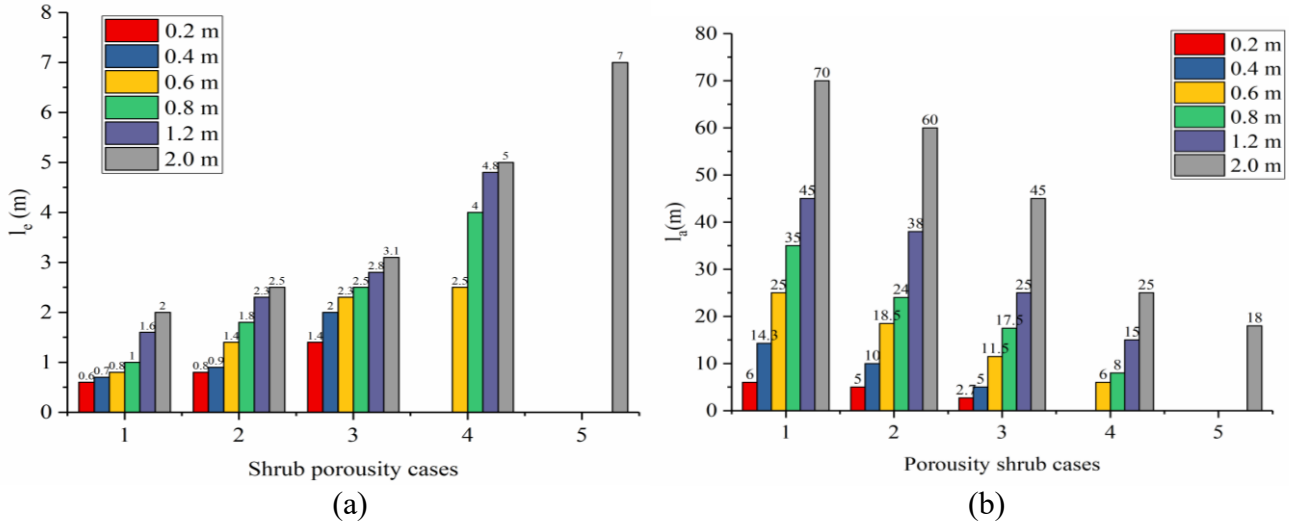

Fig. 8: (a) Shrub height and I erosion zone length l_e (b) Shrub height and sedimentation zone length (m).

Table 2: Shrub height with the corresponding number for Fig. 7.

Case number	1	2	3	4	5	6
Shrub height	0.2	0.4	0.6	0.8	1.3	2

Table 3: Shrub porosity with the corresponding number for Fig. 8.

Case number	1	2	3	4	5
Porosity %	15	30	40	50	60

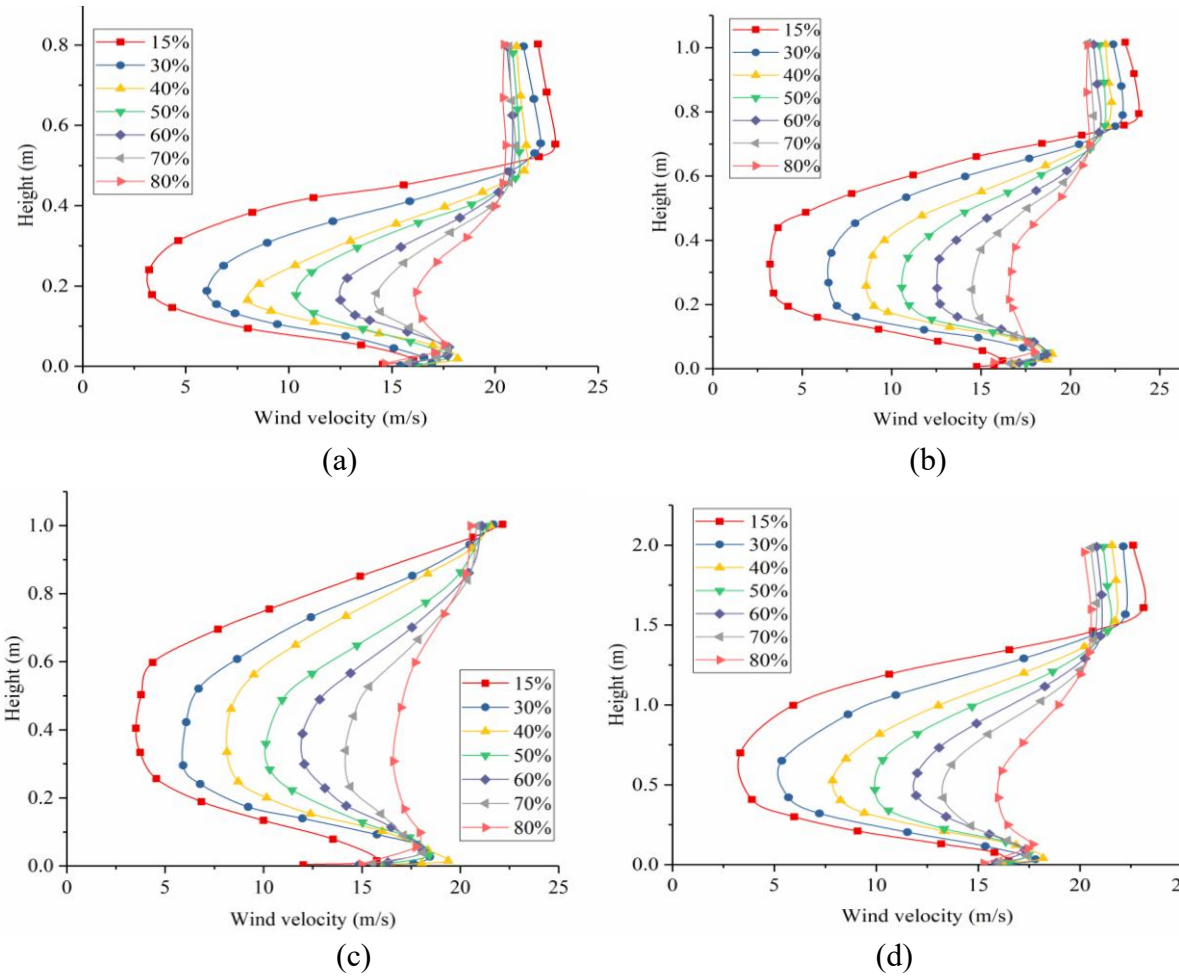

Fig. 9: Vertical wind velocity at x =0.1 m (a) Shrub height 0.4 m (b) Shrub height 0.6 m (c) Shrub height 0.8 m (d) Shrub height 1.2 m.

downstream of the fourth row, a fifth row was added at a distance of 5 m. Although, double and triple rows of shrub with 80 % porosity resulted in 30 % and 40 % wind velocity reduction (Fig.11). However, the wind velocity exceeds the threshold friction velocity of desert regions. The four rows of shrubs with 80 % porosity consequently resulted in a 50 % wind velocity reduction. Therefore, the sedimentation zone is generated from a relative distance of 3 m from the first row of the shrub. The length of the sedimentation zone at the downstream of the fourth row is 5 m. Hence, the fifth row of the shrub plant is at a distance of 5 m away from the fourth row. No erosion zone is generated the downstream of fifth rows, and the length of the sedimentation zone the downstream of fifth rows is 5 m. therefore, the remaining rows of shrub plants with a distance of 5 m away from each other.

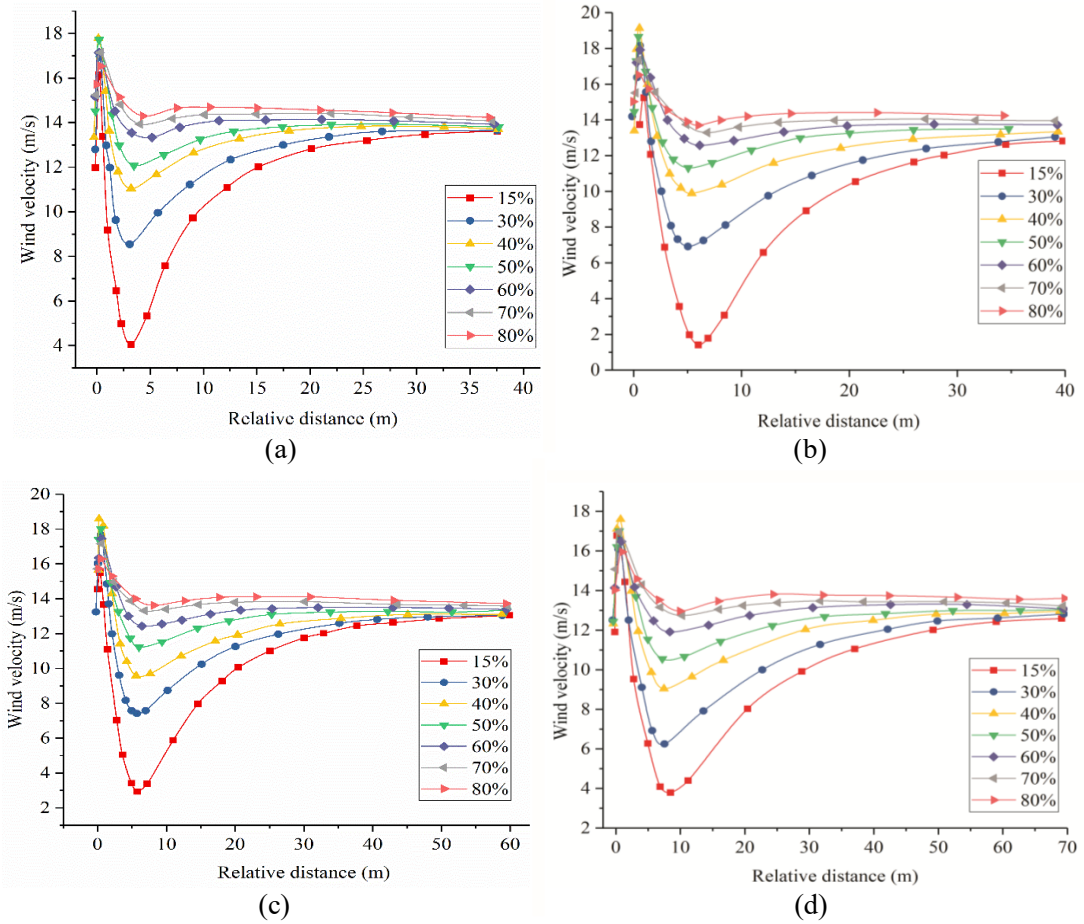

Fig. 10: Horizontal wind velocity at y=0.03 m (a) Horizontal wind velocity of shrub with 0.4 m height (b) Horizontal wind velocity of shrub with 0.6 m height (c) Horizontal wind velocity of shrub with 0.8 m height (d) Horizontal wind velocity of shrub with 1.2 m height.

From Fig. 12, can be observed that when the porosity of shrubs is 70 %, the single and double rows of shrub have wind velocity reduction. However, no sedimentation zone is generated. When the third row of shrub with 70 % porosity is added, a sedimentation zone is generated from a relative distance of 3 m from the first row with a sedimentation length zone of 5 m. Thus, it is recommended to plant the fourth row of the shrub at a distance of 5 m away from the third row.

CONCLUSION

Based on the wind tunnel measurement, and CFD simulations, the aerodynamic behavior of shrubs with different porosity, and height were studied. The downstream of shrubs were divided into three zones; the first erosion zone, the sedimentation zone, and the second erosion zone. In this study, the length of the first erosion and sedimentation zones were investigated in detail as a function of height, porosity, the number of shrub rows, and rows space.

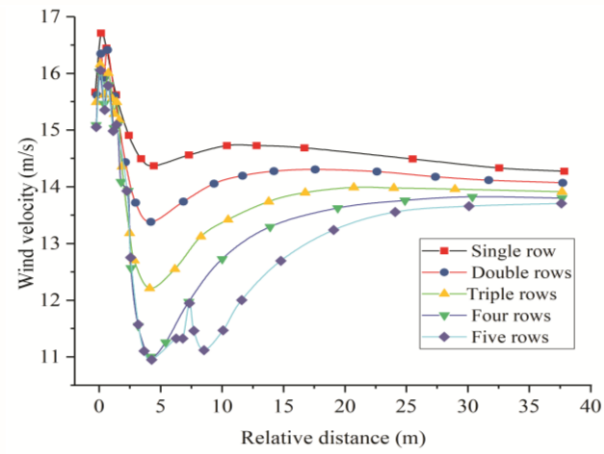

Fig. 11: Rows of shrub with 80% porosity.

The results showed that the porosity of shrubs had a significant influence on the erosion and sedimentation zones.

Table 4: Relationship between porosity, height, and first erosion zone and sediment zone length (m).

Shrub height(m)	0.2		0.4		0.6		0.8		1.2		2	
Porosity \ Zone (m)	L_e	L_a	L_e	L_a	L_e	L_a	L_e	L_a	L_e	L_a	L_e	L_a
80 %	yes	No	yes	No	yes	No	yes	No	yes	No	yes	No
70 %	yes	No	yes	No	yes	No	yes	No	yes	No	yes	No
60 %	yes	No	yes	No	yes	No	yes	No	yes	No	7	18
50 %	yes	No	yes	No	2.5	6	4	8	4.8	15	5	25
40 %	1.4	2.7	2	5	2.3	11.5	2.5	17.5	2.8	25	3.1	45
30 %	0.8	5	0.9	10	1.4	18.5	1.8	24	2.3	38	2.5	60
15 %	0.6	6	0.7	14.3	0.8	25	1	35	1.6	45	2	70

A low porous shrub had a better shelterbelt effect. With the increase in porosity, the erosion zone length increased; in contrast, the sedimentation zone length decreased. For a 20 $m.s^{-1}$ incoming critical wind velocity, if the porosity of a single row of shrub exceeded 40 %, then no sedimentation zone was generated.

Shrub height is also the main factor for wind erosion control. With the increase in shrub height, the first erosion and length of sedimentation zones also increased. Multi rows of shrubs have a better shelterbelt effect on wind erosion control, for instance, shrubs with 0.4 m height, 0.4 m rows space, and 80 % porosity, four rows of shrubs were needed to generate a sedimentation zone, which makes a 5 m long shelterbelt. In this case, the space between the remaining shrubs ' rows could be chosen as 5 m. While for a 0.4 m height shrub with 70 % porosity, three rows of shrubs were needed to make a 5 m long shelterbelt, and the distance between the remaining rows of shrubs could be chosen as 5 m. Hence, to make a better shelter zone, it is recommended to plant denser shrubs rows at upstream and sparsely shrubs rows at far downstream.

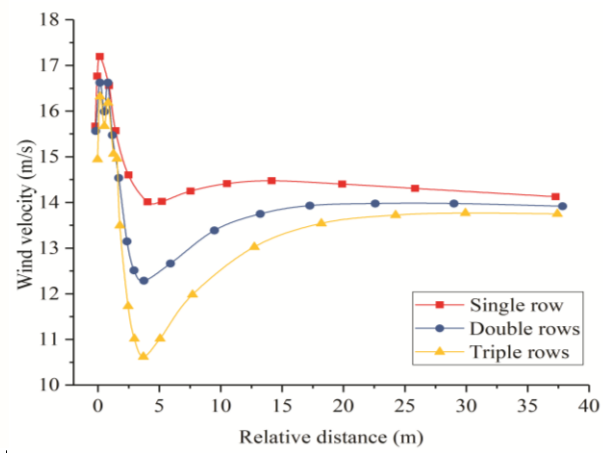

Fig. 12: Rows of shrub with 70% porosity.

REFERENCES

Ash, J. and Wasson, R. 1983. Vegetation and sand mobility in the Australian desert dunefield. Zeitschrift fur Geomorphol., 45(Supp.): 7-25.

Bitog, J., Lee, I., Hwang, H., Shin, M., Hong, S., Seo, I., Mostafa, E. and Pang, Z. 2011. A wind tunnel study on aerodynamic porosity and windbreak drag. Forest Sci. Technol., 7(1): 8-16.

Bitog, J., Lee, I., Shin, M., Hong, S., Hwang, H., Seo, I., Yoo, J., Kwon, K., Kim, Y. and Han, J. 2009. Numerical simulation of an array of fences in Saemangeum reclaimed land. Atmos. Environ., 43(30): 4612-4621.

Bo, T., Ma, P. and Zheng, X. 2015. Numerical study on the effect of semi-buried straw checkerboard sand barriers belt on the wind speed. Aeol. Res., 16: 101-107.

Cheng, J., Xin, G., Zhi, L. and Jiang, F. 2017. Unloading characteristics of sand-drift in wind-shallow areas along the railway and the effect of sand removal by force of the wind. Sci. Rep., 7(1): 1-11.

Cornelis, W. and Gabriels, D. 2005. Optimal windbreak design for wind-erosion control. J. Arid Environ., 61(2): 315-332.

Dong, Z., Mu, Q. and Liu, X. 2007. Defining the threshold wind velocity for moistened sediments. J. Geophys. Res. Solid Earth, 112(B8): 651.

Gao, Y., Qiu, G., Ding, G., Hideyuki, S., Yi, Y., Hu, C., Liu, Y., Tobe, K., Wang, Y. and Wang, J. 2004. Effect of Salix psammophila checkerboard on reducing wind and stabilizing sand. J. Desert Res., 24(3): 365-370.

Griffin, D.W., Kellogg, C.A. and Shinn, E.A. 2001. Dust in the wind: long-range transport of dust in the atmosphere and its implications for global public and ecosystem health. Glob. Change Human Health, 2(1): 20-33.

Guo, L. and Maghirang, R.G. 2012. Numerical simulation of airflow and particle collection by vegetative barriers. Eng. Appl. Computat. Fluid Mech., 6(1): 110-122.

Hong, C., Chenchen, L., Xueyong, Z., Huiru, L., Liqiang, K., Bo, L. and Jifeng, L. 2020. Wind erosion rate for vegetated soil cover: A prediction model based on surface shear strength. Catena, 187: 104398.

Jian, Z., Bo, L. and Mingyue, W. 2018. Study on windbreak performance of tree canopy by numerical simulation method. J. Computat. Multiphase Flows, 10(4): 259-265.

Li, L., Li, X., Lin, B. and Zhu, Y. 2006. Simulation of canopy flows using k-epsilon two-equation turbulence model with source/sink terms. J. Tsinghua Univ., 46(6): 753.

Liu, C., Zheng, Z., Cheng, H. and Zou, X. 2018. Airflow around single and multiple plants. Agric. Forest Meteorol., 252: 27-38.

Lv, P. and Dong, Z. 2012. Study of the windbreak effect of shrubs as a function of shrub cover and height. Environ. Earth Sci., 66(7): 1791-1795.

Mochida, A., Tabata, Y., Iwata, T. and Yoshino, H. 2008. Examining tree canopy models for CFD prediction of wind environment at pedestrian level. J. Wind Eng. Indust. Aerodyn., 96(10-11): 1667-1677.

Prospero, J.M. 1999. Assessing the impact of advected African dust on air quality and health in the eastern United States. Human Ecol. Risk Assess. Int. J., 5(3): 471-479.

Qiu, G.Y., Lee, I., Shimizu, H., Gao, Y. and Ding, G. 2004. Principles of dune fixation with straw checkerboard technology and its effects on the environment. J. Arid Environ., 56(3): 449-464.

Qu, J., Zu, R., Zhang, K. and Fang, H. 2007. Field observations on the protective effect of semi-buried checkerboard sand barriers. Geomorphology, 88(1-2): 193-200.

Rosenfeld, M., Marom, G. and Bitan, A. 2010. Numerical simulation of the airflow across trees in a windbreak. Bound. Layer Meteorol., 135(1): 89-107.

Santiago, J., Martin, F., Cuerva, A., Bezdenejnykh, N. and Sanz Andrés, A. 2007. Experimental and numerical study of wind flow behind windbreaks. Atmos. Environ., 41(30): 6406-6420.

Sarkar, S., Chauhan, A., Kumar, R. and Singh, R.P. 2019. Impact of deadly dust storms (May 2018) on air quality, meteorological, and atmospheric parameters over the northern parts of India. GeoHealth, 3(3): 67-80.

Shao, Y. and Lu, H. 2000. A simple expression for wind erosion threshold friction velocity. J. Geophys. Res. Atmos., 105(D17): 22437-22443.

Station, S.D.R. 1986. The principles and measures are taken to stabilize shifting sands along the railway line in the southeastern edge of the Tengger Desert. J. Desert Res., 6(3): 1-19.

Thomas, D. 1988. The wind is a geological process on Earth, Mars, Venus, and Titan. J. Arid Environ., 15(2): 217-218.

Tsoar, H. 1994. Bagnold: The physics of blown sand and desert dunes. Prog. Phys. Geogr., 18(1): 91-96.

Wu, F. and Zhang, H. (ed.) 2012. Turang Qinshi Xue. Science Press, Beijing, China

Xu, L. 1996. Sand fixation project with forest sand barrier and its ecological benefit. J. Desert Res., 6: 11-21.

Yao, Z., Xiao, J. and Jiang, F. 2012. Characteristics of daily extreme-wind gusts along the Lanxin Railway in Xinjiang, China. Aeol. Res., 6: 31-40.

Yoshida, S. 2006. Development of Three Dimensional Plant Canopy Model for Numerical Simulation of Outdoor Thermal Environment. The 6th International Conference on Urban Climate, 2006, 12-16 July, 2006, Goteborg, Sweden.

Zhang, X. 1994. Principles and Optimal Models for Development of Maowusu Sandy Crassland. Chinese J. Plant Ecol., 18(1): 1-16.